Journal
of the American Ceramic Society

Flash sintering of highly insulating nanostructured phase-pure BiFeO$_3$

Luis A. Perez-Maqueda[1,2] | Eva Gil-Gonzalez[1] | Antonio Perejon[1,3] |
Jean-Marie Lebrun[2] | Pedro E. Sanchez-Jimenez[1] | Rishi Raj[2]

[1]Instituto de Ciencia de Materiales de Sevilla, Consejo Superior de Investigaciones Científicas, Universidad de Sevilla, Sevilla, Spain

[2]Department of Mechanical Engineering, University of Colorado at Boulder, Boulder, Colorado

[3]Departamento de Química Inorgánica, Facultad de Química, Universidad de Sevilla, Sevilla, Spain

Correspondence
Luis A. Perez-Maqueda, Instituto de Ciencia de Materiales de Sevilla, Consejo Superior de Investigaciones Científicas, Universidad de Sevilla, Sevilla, Spain
Email: maqueda@cica.es

Present address
Jean-Marie Lebrun, Saint-Gobain Innovative Materials - NRDC, Process Technology CRL - Forming & 3D Printing Group, Northboro, Massachusetts

Abstract

We show that BiFeO$_3$, that is electrically homogeneous, is a good insulator, and has a low dielectric constant (the properties desired in its applications), can be produced by flash sintering, which is nominally difficult to achieve by conventional and spark plasma sintering processes. The flash-sintered specimens had a uniform microstructure with a nanometric grain size of ~20 nm.

KEYWORDS
BiFeO$_3$, electrically homogeneous, flash sintering, high purity, insulating, nanostructured

1 | INTRODUCTION

Bismuth iron oxide is a multiferroic material having applications in data storage and magnetoelectric sensors.[1-3] Nevertheless, most conventionally prepared materials have high leakage current densities that limit their applications. This high leakage current has been associated of secondary phases,[4-7] the generation of oxygen vacancies, the loss of bismuth, or the reduction of Fe^{3+}.[8-10] Obtaining stoichiometric high purity and dense pellets of BiFeO$_3$ is quite challenging as this compound decomposes at relatively low temperatures producing undesirable phases.[11-14] Thus, conventional sintering, which requires high temperatures and long treatments, often produces nonstoichiometric compounds with high leakage currents. Spark plasma sintering (SPS)[15-22] yields high-density BiFeO$_3$, but the highly reducing conditions produced by the graphite dies cause reduction of the sample and an increase in the electrical conductivity.[20,21]

Flash sintering was first applied to 3 mol% yttria-stabilized tetragonal zirconia.[23] Different compounds have been sintered in this way.[24-27] In the present work, we explore

the application of flash sintering and its effect on the electrical properties of $BiFeO_3$. We are able to sinter $BiFeO_3$, which not only has high density but also is single phase with a nanoscale grain size, and has desirable electrical properties, including insulating behavior.

2 | EXPERIMENTAL METHODS

In the present work, nanoscale powders of $BiFeO_3$ were synthesized by milling the stoichiometric amounts of the single commercial oxides, that is, Fe_2O_3 (Sigma-Aldrich 310050 [St. Louis, MO, USA], ≥99% purity) and Bi_2O_3 (Sigma-Aldrich 223891, 99.9% purity), using a high-energy planetary ball mill (Fritsch Pulverisette 7, Fritsch GmbH, Idar-Oberstein, Germany) under 7 bar of oxygen pressure.[28]

Flash-sintering experiments were performed using the standard procedure.[23] The powders were uniaxially pressed at 500 MPa into dog-bone shaped pellets. The samples were suspended into a tubular furnace by means of two platinum wires attached to the handles of the dog bone. The furnace was heated from room temperature at a constant rate of $10°C·min^{-1}$ up to flash event. A DC electric field was applied through the two platinum wires using a DC power supply. The field was held constant up to the point of the flash event, which was signaled by a nonlinear rise in conductivity. The voltage control at the power supply was switched to current control when the current reached a preset limit. Constant current was held for 15 seconds before the power supply to the specimen was switched off. The furnace was then allowed to cool down to room temperature. The change in the sample dimensions was monitored with a CCD camera. These data were used to measure the linear shrinkage arising from sintering.

X-ray diffraction patterns were recorded with a Panalytical X'Pert Pro diffractometer (Panalytical B.V., Almelo,

the Netherlands). Sample microstructure was analyzed by scanning electron microscopy (SEM) using a Hitachi S-4800 instrument (Hitachi, Ltd., Tokyo, Japan) equipped with energy-dispersive X-ray spectrometer (EDX). Impedance spectroscopy measurements of Au sputter-coated samples were performed, taking into account the blank capacitance of the sample holder and the overall pellet geometry, in a Newtons4th Ltd. (Leicester, UK) impedance analyzer over the frequency range from 100 Hz to 1 MHz, with AC measuring voltage of 0.1 V.

3 | RESULTS

Plots of the power dissipation, which is equal to the product of the electric field and the current density, are shown in Figure 1A. The rise in current under voltage control signals the onset of the flash. The peak in the power density occurs when the power supply is switched to current control. The plateau thereafter corresponds to the steady state of flash. The sample sinters near the power peak. The specimen temperature at the power peak can be calculated from the blackbody radiation model[29]; these values, which have been derived in the Supporting Information, are shown as T_{BBR} in the figure. The shrinkage data are shown in Figure 1B. The 0 V data represent conventional sintering. At $15 V·cm^{-1}$, the sintering behavior remains the same as in conventional sintering. At $50 V·cm^{-1}$ and above, the sample sinters by the flash mechanism. As the field is increased, sintering occurs at a lower temperature, for example, at $150 V·cm^{-1}$, the sample sinters at a furnace temperature of ~400°C.

The diffraction patterns of sintered specimens are given in Figure 1C. The retention of pure $BiFeO_3$ perovskite phase under flash sintering is indeed noteworthy. Conventionally sintered $BiFeO_3$ decomposes into secondary phases.
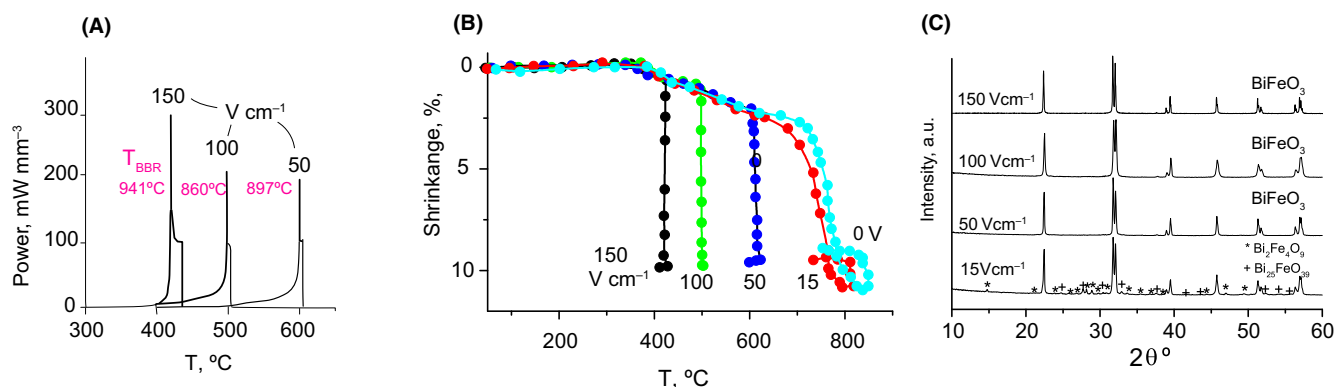

FIGURE 1 A, Power dissipation and (B) linear shrinkage as a function of furnace temperature at constant heating rate of $10°C·min^{-1}$ for different applied fields. Specimen temperatures, T_{BBR}, at the power peak have been calculated from the blackbody radiation model. C, X-ray diffraction patterns of the resulting pellets obtained from experiments at different applied fields. 0 and $15 V·cm^{-1}$ patterns resulted very similar, so only the $15 V·cm^{-1}$ is shown [Color figure can be viewed at wileyonlinelibrary.com]

The microstructure of the specimen flashed at 100 V·cm^{-1} and 20 mA·mm^{-2} is shown in Figure 2. The specimen is well sintered with low porosity. A histogram of the grain-size distribution showing an average grain size of 20±6 nm is also shown in Figure 2. The chemical composition of the sample, as determined by EDX, is given in Table S1. There is no loss of bismuth under flash-sintering conditions.

The electrical properties of the specimens were measured by impedance spectroscopy for the sample that was
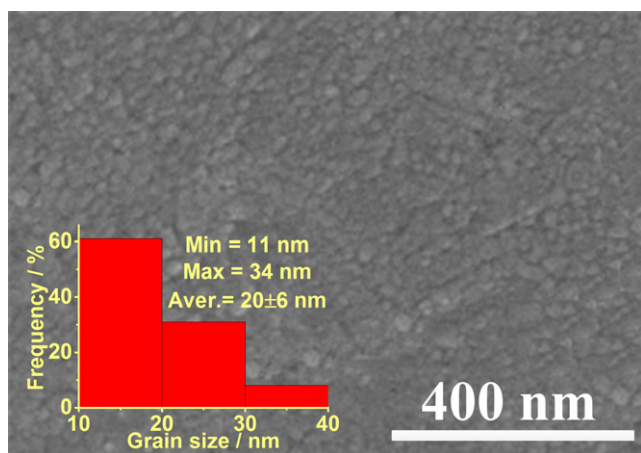
flashed at 100 V·cm^{-1}, with a current limit of 20 mA·mm^{-2}. The measurements were done with a frequency range of 100 Hz to 1 MHz at 0.1 V. The impedance plots, giving the real and imaginary parts, are given in Figure 3A, which includes SPS data for comparison. The graph highlights the much higher resistance of the flash-sintered sample. The inset in Figure 3A, giving the data for the SPS sample, shows two arcs, one from grain boundaries and the other from grain matrix.[20,21] In contrast, the flashed sample shows a single arc, suggesting no difference between grain-boundary and grain-matrix resistivity. Arrhenius plots of the conductivity for flash-sintered and SPS specimens are shown in Figure 3B.[20,21] The flash-sintered specimens are more insulating. The activation energy of flash-sintered samples was 1.01 eV; the value for high-quality single crystals has been reported as 1.3 eV.[30] The measurements of conductivity by impedance spectroscopy are compared with the change in conductivity of the powder specimen during the constant heating rate flash-sintering experiment at a field of 100 V·cm^{-1} in Figure S1. Surprisingly, the conductivity of the porous specimens is higher than the impedance measurements by about an order of magnitude, which it is contrary to the expectation that pores and interparticle interfaces would lower the conductivity.[31] Perhaps the difference is related to nonlinear effects under the much higher fields used in the flash experiments than in impedance spectroscopy.
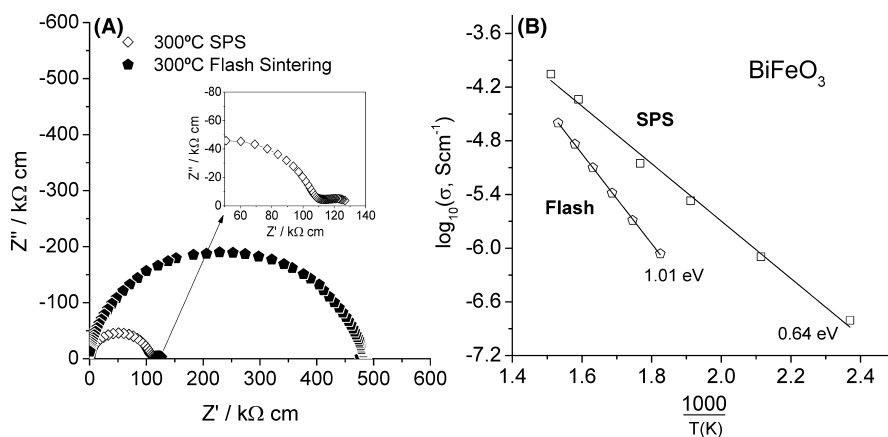

FIGURE 2 SEM micrograph and histogram plot of the grain-size distribution for BiFeO$_3$ (100 V·cm^{-1}, 20 mA·mm^{-2}) [Color figure can be viewed at wileyonlinelibrary.com]

FIGURE 3 A, Impedance complex plane plots, showing the imaginary part (Z″) vs the real part (Z′) of the impedance at 300°C for FS and SPS BiFeO$_3$. B, Bulk Arrhenius plots for FS and SPS BiFeO$_3$
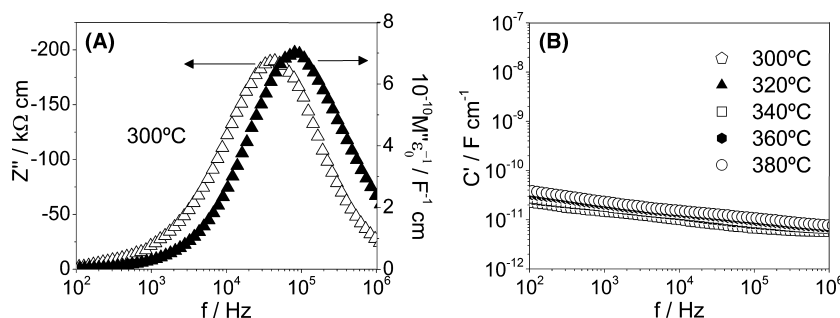

FIGURE 4 A, Z″/M″ spectroscopic plots at 300°C and (B) C′ vs frequency for BiFeO$_3$ flash-sintered sample

The imaginary parts of the modulus, M'', and the impedance, Z'', as a function of frequency at 300°C for flash-sintered $BiFeO_3$ are plotted in Figure 4. They represent Debye peaks that reflect on the electrical homogeneity of the sample. The ideal RC element with the shape of a single Debye peak indicates a homogeneous material.[32] In the present case, M'' and Z'' show single peaks with a small displacement in their frequency maxima, as shown in Figure 4A. These results show that the flash-sintered sample was electrically homogeneous.

The capacitance values calculated from the imaginary part of the impedance are shown in Figure 4B. The permittivity was calculated to be equal to 113; it was obtained by dividing the capacity by the permittivity of free space. Capacitance, equal approximately to ~10 pF·cm^{-1}, remains reasonably constant within the entire frequency range, again confirming that the sample was electrically homogeneous.[32]

4 | DISCUSSION

It is clear from above results that flash sintering helps to preserve the phase purity and compositional fidelity in (complex) ceramic oxides which are otherwise prone to decomposition and volatilization. Since sintering requires mass transport, its rate is controlled by the slowest diffusing species in the solid state, which may require temperatures where low melting and volatile species may be difficult to retain. However, it may be rather simplistic to imagine that lower (furnace) sintering temperatures and shorter sintering time afforded by flash sintering can of themselves alleviate this issue. Flash sintering has complexity, and its role in obtaining unusual results may not be reduced to rather simple arguments. For example, while in the present case flash preserves the phase fidelity, there are examples where metastable phases can form during the flash-sintering experiments, for example, in the yttria-stabilized zirconia system,[33] and more recently, in the alumina-magnesium aluminate system.[34] A fuller understanding of the how phase transitions and composition fidelity are influenced not only by time, temperature, and environment, but also by electrical field and current, during flash experiments, is far from complete.

5 | CONCLUSIONS

Flash sintering enables the processing of $BiFeO_3$ into a pure perovskite, single phase structure, which is hard to obtain in conventional sintering as the material is unstable at temperatures required for processing. Moreover, high-density nanostructured ceramics with narrow grain-size distribution were obtained. The conductivity of flash-sintering specimens was nearly one order of magnitude lower than samples made by SPS.

REFERENCES

1. Andrew JS, Starr JD, Budi MAK. Prospects for nanostructured multiferroic composite materials. *Scripta Mater.* 2014;74:38-43.
2. Eerenstein W, Mathur ND, Scott JF. Multiferroic and magneto-electric materials. *Nature*. 2006;442:759-765.
3. Roy A, Gupta R, Garg A. Multiferroic memories. *Adv Cond Matter Phys.* 2012;2012: Article ID 926290.
4. Muneeswaran M, Dhanalakshmi R, Giridharan NV. Structural, vibrational, electrical and magnetic properties of $Bi_{1-x}Pr_xFeO_3$. *Ceram Int.* 2015;41:8511-8519.
5. Wang YP, Zhou L, Zhang MF, Chen XY, Liu JM, Liu ZG. Room-temperature saturated ferroelectric polarization in $BiFeO_3$ ceramics synthesized by rapid liquid phase sintering. *Appl Phys Lett.* 2004;84:1731-1733.
6. Das SR, Choudhary RNP, Bhattacharya P, et al. Structural and multiferroic properties of La-modified $BiFeO_3$ ceramics. *J Appl Phys.* 2007;101:034104.
7. Yuan GL, Or SW, Wang YP, Liu ZG, Liu JM. Preparation and multi-properties of insulated single-phase $BiFeO_3$ ceramics. *Solid State Commun.* 2006;138:76-81.
8. Pabst GW, Martin LW, Chu YH, Ramesh R. Leakage mechanisms in $BiFeO_3$ thin films. *Appl Phys Lett.* 2007;90:072902.
9. Qi X, Dho J, Tomov R, Blamire MG, MacManus-Driscoll JL. Greatly reduced leakage current and conduction mechanism in aliovalent-ion-doped $BiFeO_3$. *Appl Phys Lett.* 2005;86:1-3.
10. Yang H, Jain M, Suvorova NA, et al. Temperature-dependent leakage mechanisms of $Pt/BiFeO_3/SrRuO_3$ thin film capacitors. *Appl Phys Lett.* 2007;91:072911.
11. Maitre A, Francois M, Gachon JC. Experimental study of the $Bi_2O_3–Fe_2O_3$ pseudo-binary system. *J Phase Equilib Diff.* 2004;25:59-67.
12. Palai R, Katiyar RS, Schmid H, et al. Beta phase and gamma-beta metal-insulator transition in multiferroic $BiFeO_3$. *Phys Rev B.* 2008;77:014110.
13. Lu J, Qiao LJ, Fu PZ, Wu YC. Phase equilibrium of $Bi_2O_3–Fe_2O_3$ pseudo-binary system and growth of $BiFeO_3$ single crystal. *J Cryst Growth.* 2011;318:936-941.
14. Perejon A, Sanchez-Jimenez PE, Criado JM, Perez-Maqueda LA. Thermal stability of multiferroic $BiFeO_3$: kinetic nature of the beta-gamma transition and peritectic decomposition. *J Phys Chem C.* 2014a;118:26387-26395.
15. Wang LC, Wang ZH, He SL, et al. Enhanced magnetization and suppressed current leakage in $BiFeO_3$ ceramics prepared by spark

plasma sintering of solgel derived nanoparticles. *Physica B: Condens Matter*. 2012;407:1196-1202.

16. Correas C, Hungría T, Castro A. Mechanosynthesis of the whole $xBiFeO_3$-(1 - X)$PbTiO_3$ multiferroic system: structural characterization and study of phase transitions. *J Mater Chem*. 2011;21:3125-3132.

17. Dai Z, Akishige Y. Electrical properties of multiferroic $BiFeO_3$ ceramics synthesized by spark plasma sintering. *J Phys D: Appl Phys*. 2010;43:445403.

18. Mazumder R, Chakravarty D, Bhattacharya D, Sen A. Spark plasma sintering of $BiFeO_3$. *Mater Res Bull*. 2009;44:555-559.

19. Jiang QH, Nan CW, Wang Y, Liu YH, Shen ZJ. Synthesis and properties of multiferroic $BiFeO_3$ ceramics. *J Electroceram*. 2008;21:690-693.

20. Perejon A, Sanchez-Jimenez PE, Poyato R, et al. Preparation of phase pure, dense fine grained ceramics by conventional and spark plasma sintering of La-substituted $BiFeO_3$ nanoparticles. *J Eur Ceram Soc*. 2015;35:2283-2293.

21. Perejon A, Maso N, West AR, et al. Electrical properties of stoichiometric $BiFeO_3$ prepared by mechanosynthesis with either conventional or spark plasma sintering. *J Am Ceram Soc*. 2013;96:1220-1227.

22. Song SH, Zhu QS, Weng LQ, Mudinepalli VR. A comparative study of dielectric, ferroelectric and magnetic properties of $BiFeO_3$ multiferroic ceramics synthesized by conventional and spark plasma sintering techniques. *J Eur Ceram Soc*. 2015;35:131-138.

23. Cologna M, Rashkova B, Raj R. Flash sintering of nanograin zirconia in < 5 s at 850 degrees C. *J Am Ceram Soc*. 2010;93:3556-3559.

24. Candelario VM, Moreno R, Todd RI, Ortiz AL. Liquid-phase assisted flash sintering of SiC from powder mixtures prepared by aqueous colloidal processing. *J Eur Ceram Soc*. 2017;37:485-498.

25. Gaur A, Sglavo VM. Flash sintering of (La, Sr)(Co, Fe)O_3-Gd-doped CeO_2 Composite. *J Am Ceram Soc*. 2015;98:1747-1752.

26. Shomrat N, Baltianski S, Randall CA, Tsur Y. Flash sintering of potassium-niobate. *J Eur Ceram Soc*. 2015;35:2209-2213.

27. Zhang Y, Luo J. Promoting the flash sintering of ZnO in reduced atmospheres to achieve nearly full densities at furnace temperatures of <120°C. *Scripta Mater*. 2015;106:26-29.

28. Perejon A, Sanchez-Jimenez PE, Perez-Maqueda LA, et al. Single phase, electrically insulating, multiferroic La-substituted $BiFeO_3$ prepared by mechanosynthesis. *J Mat Chem C*. 2014b;2:8398-8411.

29. Raj R. Joule heating during flash-sintering. *J Eur Ceram Soc*. 2012;32:2293-2301.

30. Catalan G, Scott JF. Physics and applications of bismuth ferrite. *Adv Mater*. 2009;21:2463-2485.

31. Bruce PG, West AR. The A-C conductivity of polycrystalline LISICON, Li2+2xZn1-xGeO4, and a model for intergranular constriction resistances. *J Electrochem Soc*. 1983;130:662-669.

32. Irvine JTS, Sinclair DC, West AR. Electroceramics: characterization by impedance spectroscopy. *Adv Mater*. 1990;2:132-138.

33. Lebrun JM, Morrissey TG, Francis JSC, Seymour KC, Kriven WM, Raj R. Emergence and extinction of a new phase during on-off experiments related to flash sintering of 3YSZ. *J Am Ceram Soc*. 2015;98:1493-1497.

34. Kok D, Jha SK, Raj R, Mecartney ML. Flash sintering of a three-phase alumina, spinel, and yttria-stabilized zirconia composite. *J Am Ceram Soc*. 2017;1-7. https://doi.org/10.1111/jace.14818.

SUPPORTING INFORMATION

Additional Supporting Information may be found online in the supporting information tab for this article.